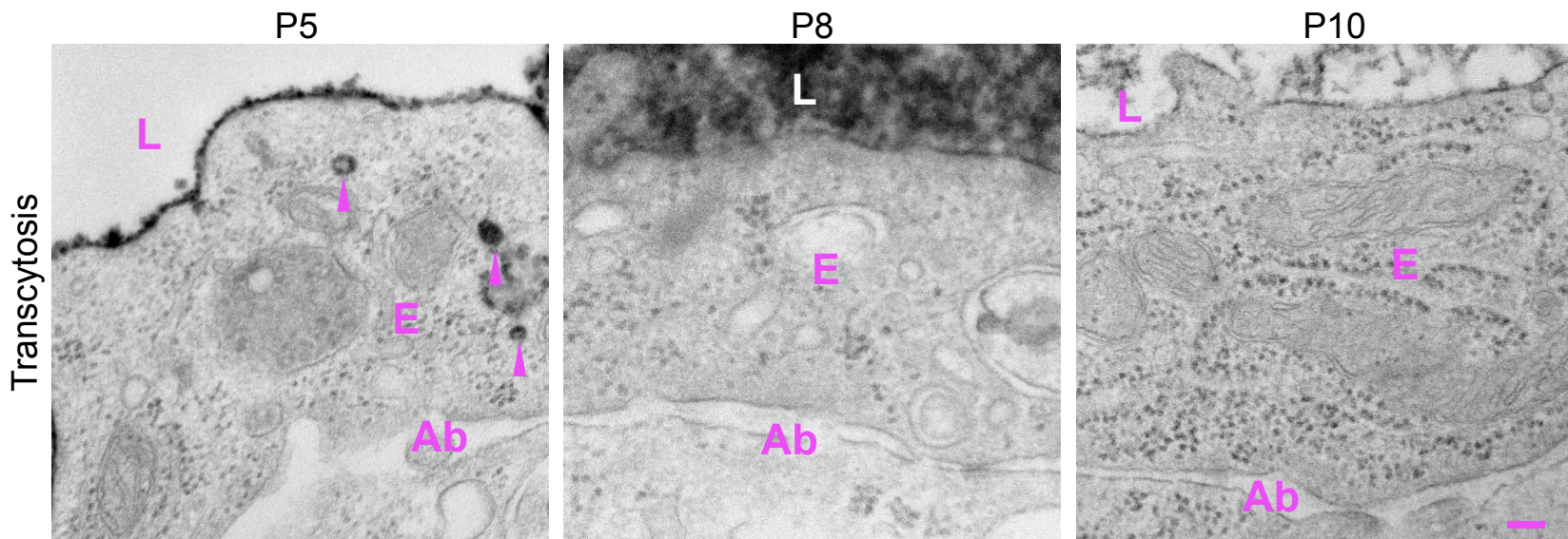
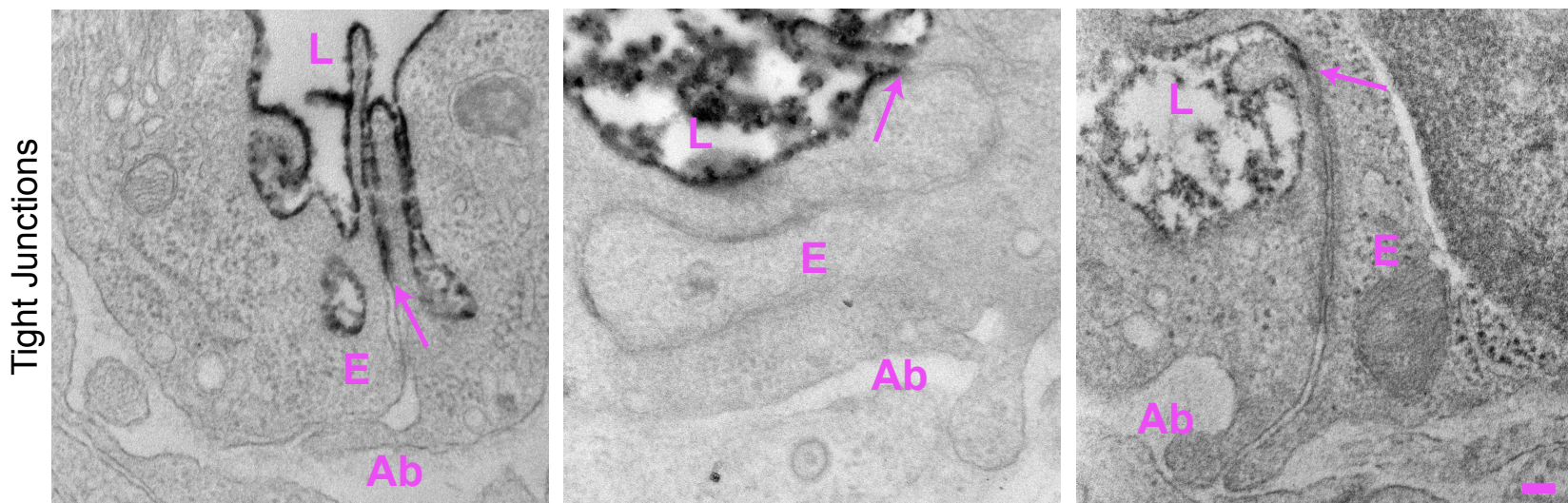


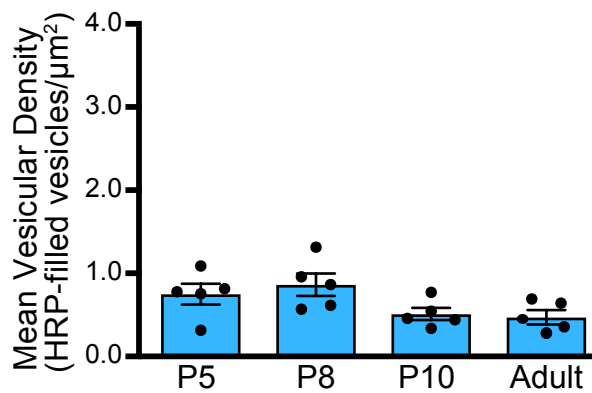
**A**



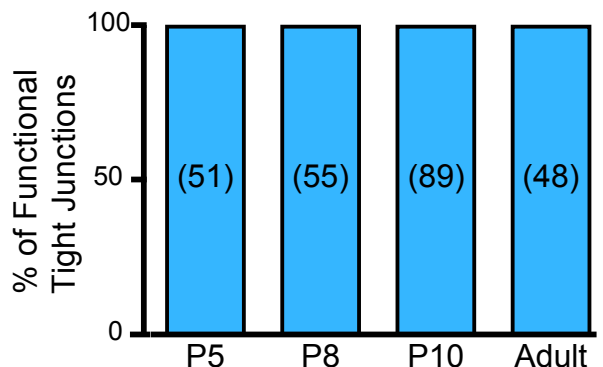
**B**

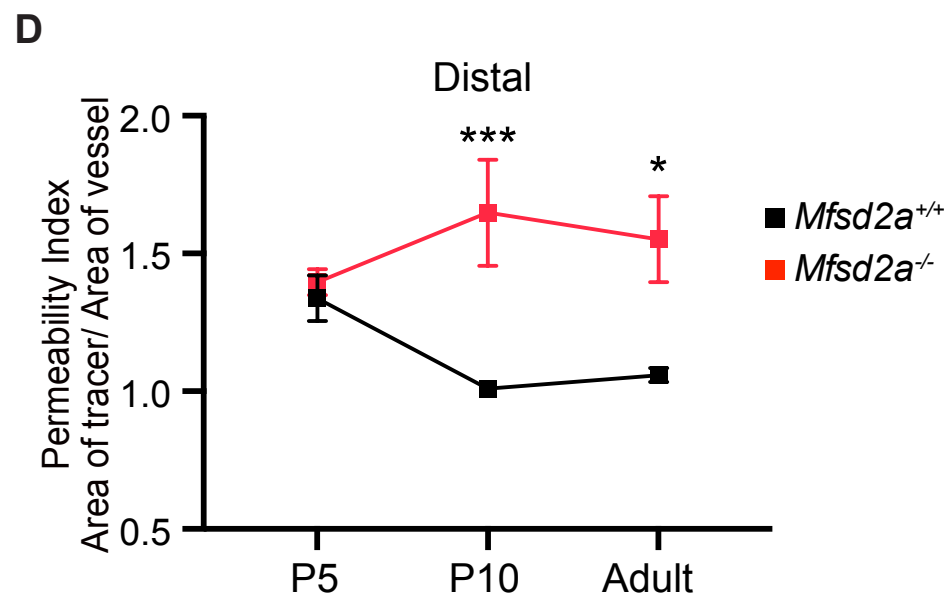
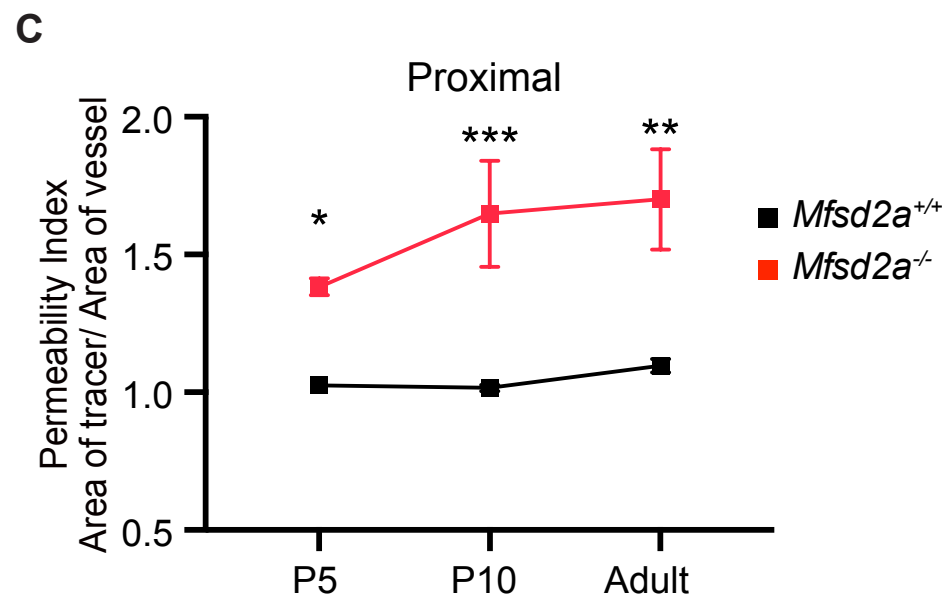
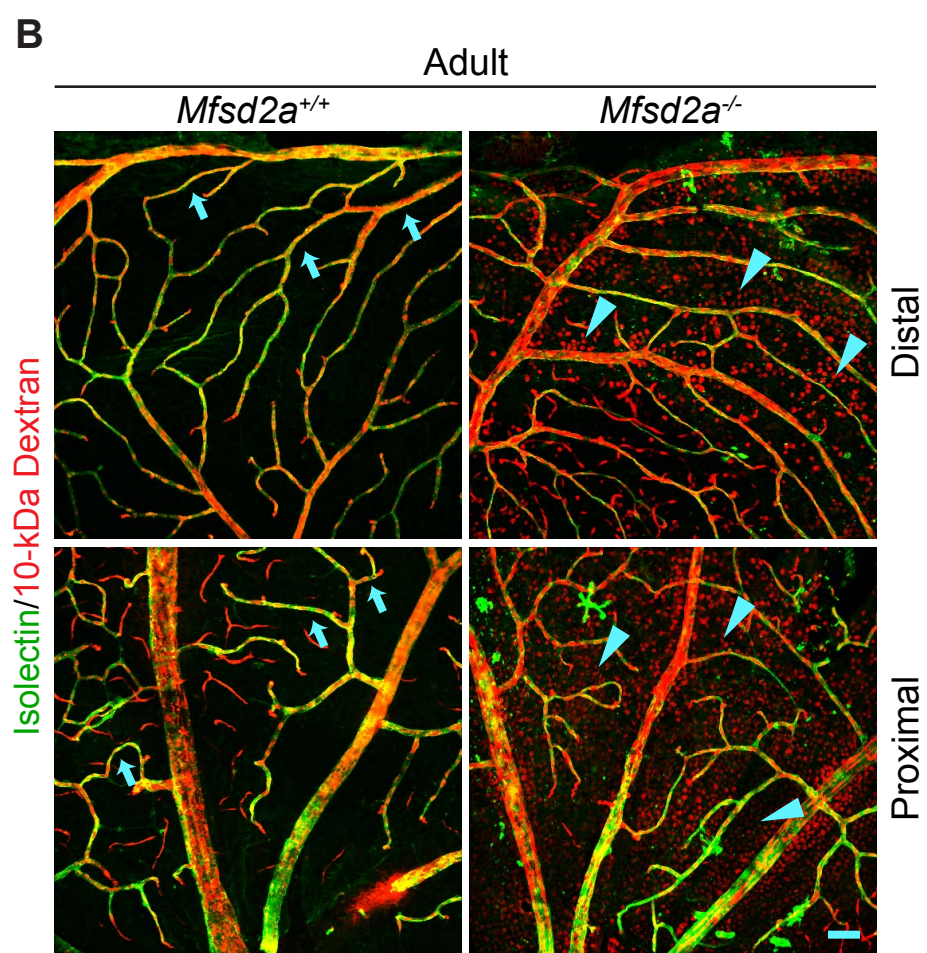
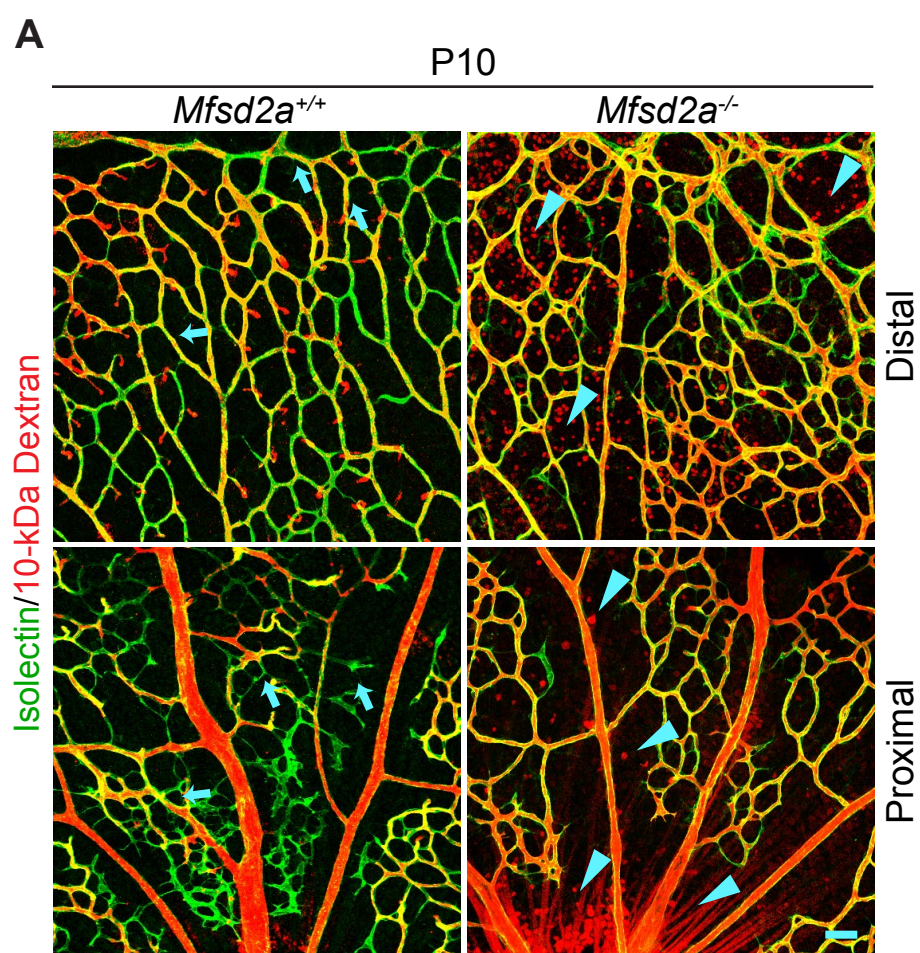


**C**



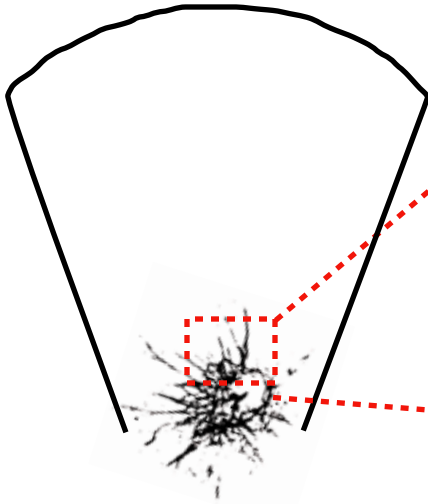
**D**



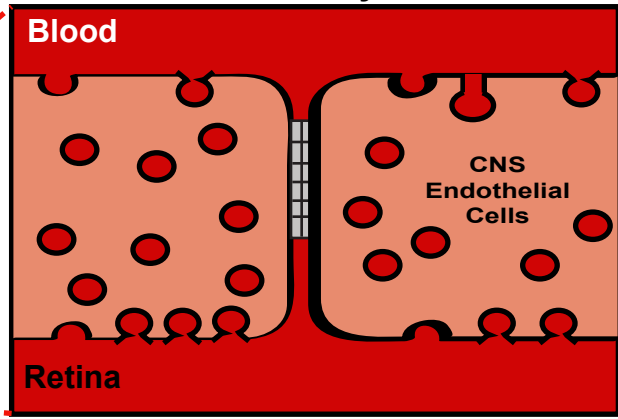


When vessels first enter the CNS

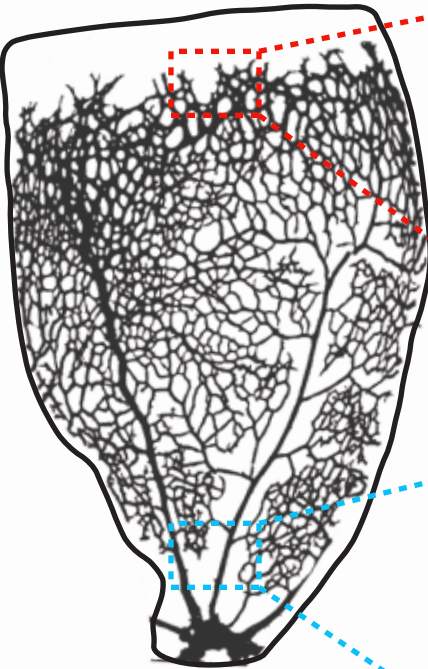
P1



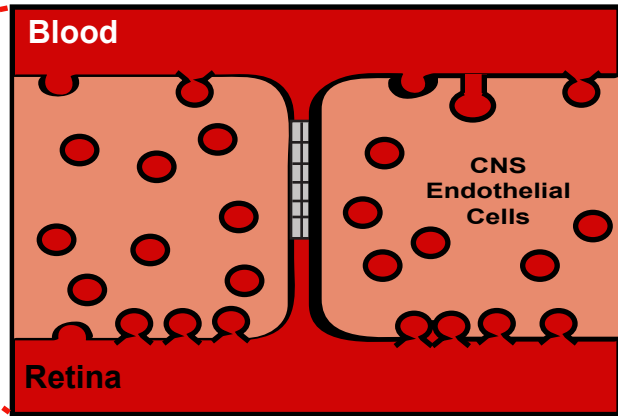
**Bulk transcytosis**



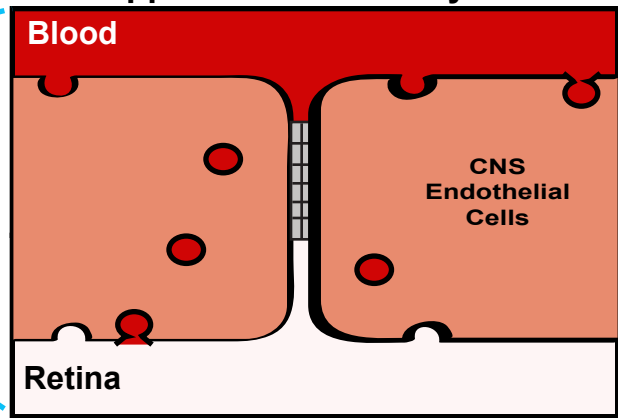
P5



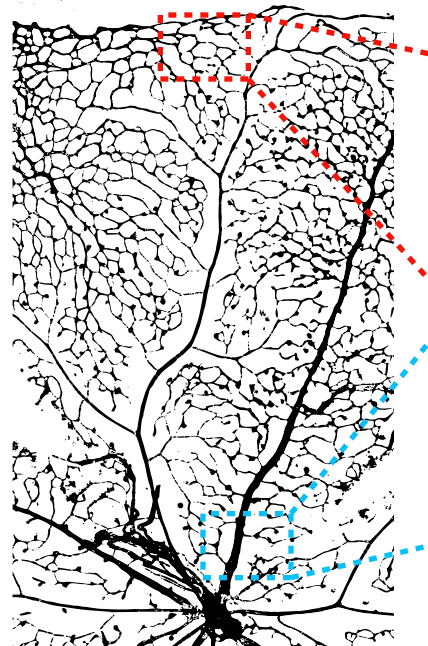
**Bulk transcytosis**



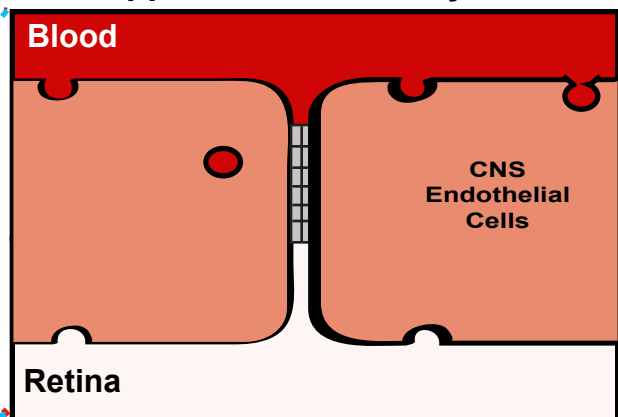
**Suppression of transcytosis**



P10



**Suppression of transcytosis**



1 **Supplemental Figure Legends:**

2 **Figure S1. Characterization of functional BRB in adult retinal vasculature and developing proximal,**  
3 **deeper plexus and intermediate plexus vessels. Related to Figure 1. (A)** In a functional adult BRB, the  
4 vessels (isolectin; green) of the primary (1<sup>st</sup> and 2<sup>nd</sup> row), intermediate (3<sup>rd</sup> row) and deeper plexus (4<sup>th</sup> row)  
5 completely confines (arrow) both the Sulfo-NHS-Biotin (left) and 10-kDa dextran (right) tracers (red). **(B)**  
6 Intravenous injections of Sulfo-NHS-Biotin (left) and 10-kDa dextran (right) tracer in postnatal mice  
7 demonstrate that the proximal vessels (green) already confine the tracer. **(C)** Quantification of the permeability  
8 index of the proximal vessels. Data are presented as mean  $\pm$  s.e.m. (n = 5-8 pups per age, from 3 different  
9 litters). Statistical significance was determined by one-way ANOVA, followed by post-hoc Bonferroni multiple  
0 comparison adjustment, comparing the various neonatal ages with the adult in the respective Sulfo-NHS-Biotin  
1 and 10-kDa dextran group. No significance was observed in the comparison of the proximal vessels. **(D)**  
2 Intravenous injections of Sulfo-NHS-Biotin (left) and 10-kDa dextran (right) tracer in postnatal mice  
3 demonstrate that sprouting deeper plexus vessels exhibit tracer leakage at P8 and P9 but not at P10. **(E)**  
4 Quantification of the permeability index of the deeper plexus vessels. Data are presented as mean  $\pm$  s.e.m. (n =  
5 5-8 pups per age, from 3 different litters). Statistical significance was determined by one-way ANOVA,  
6 followed by post-hoc Bonferroni multiple comparison adjustment, comparing the various neonatal ages with the  
7 adult in the respective Sulfo-NHS-Biotin and 10-kDa dextran group. **(F)** Sprouting intermediate plexus vessels  
8 completely confine the tracer as early as P12. **(G)** Quantification of the permeability index of the deeper plexus  
9 vessels. Data are presented as mean  $\pm$  s.e.m. (n = 5-8 pups per age, from 3 different litters). Statistical  
0 significance was determined by one-way ANOVA, followed by post-hoc Bonferroni multiple comparison  
1 adjustment, comparing the various neonatal ages with the adult in the respective Sulfo-NHS-Biotin and 10-kDa  
2 dextran group. No significance was observed in the comparison of intermediate plexus vessels. \*, P < 0.05, \*\*,  
3 P < 0.01. \*\*\*, P < 0.01. Scale bar represents 50  $\mu$ m for all panels.

4

5

6

1 **Figure S2. Pericyte coverage is constant throughout the retina, including distal leaky vessels during BRB**  
2 **development. Related to Figure 1.**

3 (A) As early as vessel ingression at P1, pericytes (NG2:DsRed; red) are already ensheathing budding CNS  
4 vessels (isolectin; green and ERG for endothelial nuclei; white). (B-D) At P5, pericyte density (C)  
5 (NG2:DsRed+ soma/ ERG1/2/3+ cells) and (D) pericyte coverage (NG2:DsRed area/Isolectin area) is around  
6 1:1 throughout the retinal vasculature, including the distal, nascent vessels. Data are presented as mean  $\pm$  s.e.m.  
7 (n = 5). The ticks in (B) represent the distance in microns from the ONH. 0 is set slightly before the ONH. (E)  
8 Pericytes are present in nascent, distal vessels yet Mfsd2a is absent in P5 retinas. The angiogenic front is  
9 outlined in blue (determined by isolectin staining). Scale bar represents 100  $\mu$ m for all panels.

1 **Figure S3. EM analysis of Proximal Vessels at P5, P8, P10 and Adult. Related to Figure 2.**

2 (A) P5 to P10 proximal endothelial cells already contain a negligible number of vesicles. (B) EM analysis of  
3 proximal vessels from P5, P8 and P10 retinas reveals tracer product halts abruptly at the tight junctions  
4 (arrows). (C) Quantifications of tracer-filled vesicular densities in the proximal endothelial cells at P5, P8 and  
5 P10. Data are presented as mean  $\pm$  s.e.m. (n= 5 mice per age; each circle represents the average vesicular  
6 density from 15 – 20 vessels per mouse). Statistical significance was determined by one-way ANOVA,  
7 followed by post-hoc Bonferroni multiple comparison adjustment, comparing the proximal vessels of the  
8 various neonatal ages to the proximal vessels of the adult. No significant difference was observed in the  
9 comparisons of the proximal vessels. (D) Quantification of the number of tight junctions that halt the tracers at  
0 the luminal side without parenchymal leakage over the total number of tight junctions in proximal vessels. (n =  
1 5 mice per age; 15-20 vessels analyzed per mouse; the number of tight junctions analyzed are displayed in the  
2 bars). The Adult data in Figure S2C and S2D is the same as Figure 2E and 2F. L – lumen, E – endothelial cells,

1 Ab – abluminal, RBC- red blood cell. \*\*\*,  $P < 0.001$ . Scale bar represents 100 nm for all panels.

2 **Figure S4. *Mfsd2a* is essential for functional BRB formation. Related to Figure 3.**

3 **(A and B)** Intravenous injection of tracer in P10 (A) and adult (B) *Mfsd2a*<sup>+/+</sup> mice results in confinement of the  
4 tracer throughout the vasculature (arrows) whereas tracer injection in *Mfsd2a*<sup>-/-</sup> mice results in tracer leakage  
5 into the retinal parenchyma (arrowheads) at both distal and proximal regions of the retina. **(C-D)** Quantification  
6 of the permeability of the **(C)** proximal and **(D)** distal vessels at P5, P10, and adult ages. Data are presented as  
7 mean  $\pm$  s.e.m. (n = 5,6, and 4 for wildtype P5, P10 and adult respectively and n=5, 5 and 4 for *Mfsd2a*<sup>-/-</sup> P5, P10  
8 and adult respectively). P5 proximal and distal vessel data is the same data from Figure 4H. Statistical  
9 significance was determined by comparing *Mfsd2a*<sup>-/-</sup> and *Mfsd2a*<sup>+/+</sup> littermates at the respective age using two-  
0 way ANOVA, followed by post-hoc Bonferroni multiple comparison adjustment. \*,  $P < 0.05$ , \*\*,  $P < 0.01$ , \*\*\*,  
1  $P < 0.001$ . Scale bar represents 50  $\mu$ m for all panels.

2  
3 **Figure S5. Illustration of the gradual suppression of transcytosis governs functional BRB formation.**

4 **Related to Figure 1.**

5 As early as vessel ingression at P1 (top), functional tight junctions are already formed to restrict paracellular  
6 flux between budding CNS endothelial cells. However, bulk transcytosis is present with many transcytotic  
7 vesicles in the endothelial cells, resulting in a leaky, immature barrier between the blood and retinal  
8 parenchyma. By P5 (middle), there is a spatiotemporal gradient of a functional BRB formation. The more  
9 mature, proximal vessels have both functional tight junctions and suppression of transcytosis to establish a  
0 functional barrier. However, the nascent, distal vessels have functional tight junctions but display bulk  
1 transcytosis, resulting in a leaky, immature barrier. By P10 (bottom), the entire retinal vasculature has  
2 functional tight junctions and suppressed transcytosis, resulting in a functional BRB throughout the vasculature.



## Method S1:

//This ImageJ macro quantifies the area of dye and the area of vessels in retina images taken from Olympus FV1200 (.oib files) using 0.75 NA 20x Objective.  
//The analysis may change accordingly if other microscopes and file types are used.

```
//initialize ImageJ
run("Colors...", "foreground=white background=black selection=yellow");
run("Options...", "iterations=1 count=1 black edm=Overwrite");

//choose folder with raw image files
rawdir=getDirectory("Choose Raw Data Folder");
//rchoose folder to save your dataset
resultdir=getDirectory("Choose Result Data Folder");
run("Set Measurements...", "area limit display redirect=None decimal=3");

//Batch process raw images
var f;

list=getFileList(rawdir);
for(f=0;f<list.length;f++)
{
    open(rawdir+list[f]);
    process();
}

//Saves the output as an excel file
selectWindow("Summary");
saveAs("Text", resultdir+"Result.xls");

//This macro assumes images are in z-stacks and assumes "channel one" is blood
vessel and "channel two" is tracer
function process()
{
    //max z project
    //split channels and rename
    //run("Stack to Images");
    run("Z Project...", "projection=[Max Intensity]");
    run("Subtract Background...", "rolling=100");
    run("Gaussian Blur...", "sigma=2");
    run("Split Channels");
    //Determine Vessel Area
    selectWindow("C1-MAX_"+list[f]);setAutoThreshold("Default
dark");setOption("BlackBackground", true);run("Convert to Mask");saveAs("Tiff",
resultdir+list[f]+"_Vessel_Mask.tif");run("Analyze Particles...", "size=10-Infinity
summarize");
```

```
//Determine Tracer Area
selectWindow("C2-MAX_"+list[f]);setAutoThreshold("Default
dark");setOption("BlackBackground", true);run("Convert to Mask");saveAs("Tiff",
resultdir+list[f]+"_Tracer_Mask.tif");run("Analyze Particles...", "size=10-Infinity
summarize");
run("Close All");
}
```